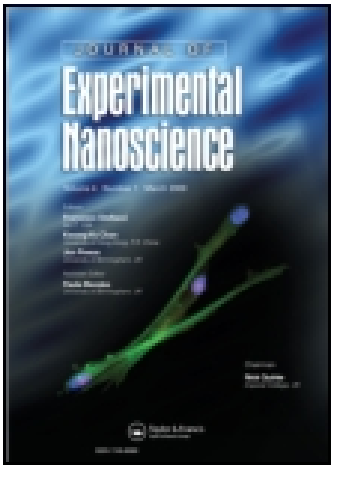

Journal of Experimental Nanoscience
Publication details, including instructions for authors and subscription information:
http://www.tandfonline.com/loi/tjen20

The growth of pine-leaf-like hierarchical SnO_2 nanostructures

Chang Fu Dee [a b], Teck Yaw Tiong [a], Binni Varghese [c], Chorng-Haur Sow [c], Yuan-Yee Wong [b], Ishaq Ahmad [d], G. Husnain [d], Edward Yi-Chang [b], Yu-Lin Hsiao [b], Hung-Wei Yu [b], Hong-Quan Nguyen [b], Muhamad Mat Salleh [a] & Burhanuddin Yeop Majlis [a]

[a] Institute of Microengineering and Nanoelectronics, Universiti Kebangsaan Malaysia , 43600 Bangi, Selangor , Malaysia

[b] Department of Material Science and Engineering , National Chiao Tung University , 1001 Ta-Hsueh Road, Hsin-Chu , Taiwan 30010 , ROC

[c] Department of Physics, Faculty of Science, 2 Science Drive 3 , National University of Singapore , Singapore 117542 , Singapore

[d] National Center for Physics , Quaid-i-Azam University , Islamabad 44000 , Pakistan

Published online: 15 Jan 2013.

To cite this article: Chang Fu Dee , Teck Yaw Tiong , Binni Varghese , Chorng-Haur Sow , Yuan-Yee Wong , Ishaq Ahmad , G. Husnain , Edward Yi-Chang , Yu-Lin Hsiao , Hung-Wei Yu , Hong-Quan Nguyen , Muhamad Mat Salleh & Burhanuddin Yeop Majlis (2014) The growth of pine-leaf-like hierarchical SnO_2 nanostructures, Journal of Experimental Nanoscience, 9:9, 913-921, DOI: 10.1080/17458080.2012.743683

To link to this article: http://dx.doi.org/10.1080/17458080.2012.743683

Journal of Experimental Nanoscience, 2014
Vol. 9, No. 9, 913–921, http://dx.doi.org/10.1080/17458080.2012.743683

Taylor & Francis
Taylor & Francis Group

The growth of pine-leaf-like hierarchical SnO_2 nanostructures

Chang Fu Dee[ab]*, Teck Yaw Tiong[a], Binni Varghese[c], Chorng-Haur Sow[c], Yuan-Yee Wong[b], Ishaq Ahmad[d], G. Husnain[d], Edward Yi-Chang[b], Yu-Lin Hsiao[b], Hung-Wei Yu[b], Hong-Quan Nguyen[b], Muhamad Mat Salleh[a] and Burhanuddin Yeop Majlis[a]

[a]*Institute of Microengineering and Nanoelectronics, Universiti Kebangsaan Malaysia, 43600 Bangi, Selangor, Malaysia;* [b]*Department of Material Science and Engineering, National Chiao Tung University, 1001 Ta-Hsueh Road, Hsin-Chu, Taiwan 30010, ROC;* [c]*Department of Physics, Faculty of Science, 2 Science Drive 3, National University of Singapore, Singapore 117542, Singapore;* [d]*National Center for Physics, Quaid-i-Azam University, Islamabad 44000, Pakistan*

(*Received 10 March 2012; final version received 16 October 2012*)

Pine-leaf-like SnO_2 hierarchical nanostructures (NSs) were grown by a two-step vapour transport deposition process with a combination of vapour–solid and vapour–liquid–solid mechanisms at the primary and secondary processes, respectively. This type of hierarchical structure consisted of SnO_2 trunk with homo-branching nanowires (NWs). The branched NWs connected the trunk NWs at included angles of 56° and 90° for two different types of hierarchical NSs. Based on the thermodynamic calculation, the formation of branched NWs at those angles are all energetically favourable.

Keywords: tin oxide; nanowire; branching; hierarchical

1. Introduction

SnO_2 is an n-type wide band gap semiconductor ($E_g = 3.6$ eV at 300 K) [1]. It could form an n-type nanostructure (NS), which is an important functional material extensively used in optical devices [2] and gas sensors [3] due to its high surface-to-volume ratio and great resistivity variation in a gaseous environment. Over the past few years, thermal evaporation method for the growth of SnO_2 with various geometrical morphologies have been reported, which includes nanowires (NWs), nanobelts, nanotubes, nanoparticles (NPs) and fish-bone-like NSs [4–8].

Until now, different approaches have been applied to alter and manipulate the properties and morphologies of NS materials and devices, such as doping [9,10], alloying [11], ion beam engineering [12–15], co-synthesising/compositing with other materials/NWs [16], surface modification [17] and plasma treatment [18]. Methods for the synthesis of branched SnO_2 NSs have also been recently developed [5]. Au-mediated growth of silicon NWs has been achieved by Dutta and Basak [16]. Hierarchical NSs have been synthesised by Cheng and other researchers through the assembly of ZnO NSs on SnO_2 trunks by a combination for solution growth and vapour transport methods. Fern-like NSs have also been obtained by Yan et al. [19]. It is believed that branched NWs could provide plenty of varieties for manipulation of nanoscaled functioning devices and building structures [20].

*Corresponding author. Email: cfdee@ukm.my

Most of the synthesis processes by vapour transport deposition (VTD) method need a vacuum system to create a low pressure or/and involved a complex deposition method. In this study, we used a two-step process for the synthesis of SnO_2 NSs by the VTD method in atmospheric pressure without the use of vacuum system. A different approach will be presented using both VTD in the primary and secondary growth processes. Compared to the solution growth method, vapour transport method has the advantage of faster growth rate. Several tens or up to more than hundreds of micrometres could be easily achieved in couple of hours. Our approach utilises a combination of vapour–solid and vapour–liquid–solid (VLS) mechanisms in the primary and secondary growth processes, respectively. The primary step for the growth of SnO_2 NWs has been achieved without the metal catalyst [21]. A secondary growth on SnO_2 NWs was carried out by sputtering of Au on SnO_2 NWs to act as a catalyst. A similar two-step process has been done by Cheng et al. [22] but with the use of hydrothermal method. However, it involved more than one approaches under different set-ups and environments (thermal and hydrothermal). This has made the growth process become more complicated.

2. Experimental details

The lateral side branching growth to form pine-leaf-like SnO_2 hierarchical NSs was achieved in two growth processes (primary and secondary) using the VTD method [23]. In the primary growth process, a clean quartz substrate was dried and sputter-coated with a SnO_2 thin film (~150 nm). This film acted as a buffer layer in the synthesis process. The source material was a mixture of purified SnO_2 powder (Sigma–Aldrich 99.9%) and graphite powder (Sigma–Aldrich 99.9%) in the ratio of 1 : 1. This mixture was placed on a ceramic plate and positioned at the centre of a mini-tube furnace. The SnO_2 thin film-coated quartz substrate was inversely positioned (the surface of the substrate was facing downward to the source) at about 1 cm above the mixed powder during the primary growth process, as shown in Figure 1. During this process, the furnace was heated up to 950°C for 1 h with a constant flow of nitrogen gas at a rate of 50 mL min^{-1}.

After the above-mentioned process, the sample was cooled down to room temperature. A layer of white product was found to have formed on the substrate. In the secondary growth process, the same substrate from the primary process was used. It was sputtered with Au (~5 nm) prior to the secondary growth process. The same parameters and experimental set-up were used. After the growth, the surface area was deposited with another layer of white product (with slightly different contrast in colour). The inner wall of the quartz tube surrounding the sample was also coated with the similar white layer of product.

Field emission scanning electron microscopy (FESEM) was used to examine the layers that were formed in the primary and secondary growth processes. Energy dispersive X-ray spectroscopy (EDS) attached with the FESEM was used to analyse the composition.

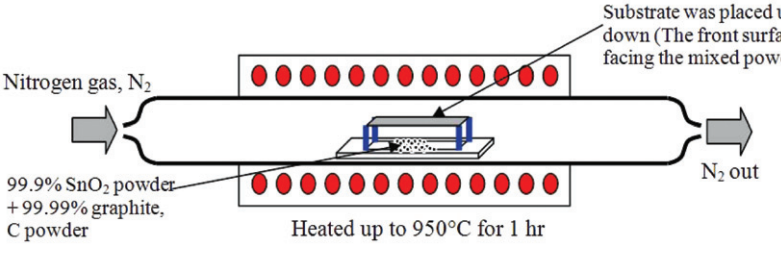

Figure 1. Schematic of the VTD method for the primary and secondary synthesis processes.

X-ray diffraction (XRD) was used to investigate the crystallinity of the NSs during both the primary and secondary processes.

3. Results and discussion

Morphologies and compositions of the sample after the primary and secondary growth processes at 950°C were analysed by FESEM and EDS (Figures 2 and 3). After 1 h of the primary growing process, SnO_2 NWs were formed on the substrate. SEM scanning (Figure 2) shows images of: (a) SnO_2 NWs after the primary growth process and (b) hierarchical NSs after the secondary growth process. After the primary growth process (Figure 2a), formation of tapered SnO_2 NWs was found. Not many NWs were formed mainly because the substrate was placed in the high supersaturated region, as described by Ye et al. [24]. Those NWs that were formed after this primary grown process served as the trunks for the growth of pine-leaf-like SnO_2 hierarchical NSs in the secondary growth process. In Figure 2(b), after the secondary growth process, the surface of the substrate was covered with whisker-like NWs. A closer examination of these hierarchical NSs is shown in Figure 3(a)–(d). Two types of hierarchical NSs could be observed. They could be differentiated by the distinct included angle with the trunk NWs. Figure 3(a) and (b) show the branched NWs connecting the trunk at an angle of ~56°. Figure 3(c) and (d) show a connecting angle of 90° with the trunk NW. Both types of branching NWs ended with a droplet at their end, provided the VLS process has taken part. It was observed that some trunk NWs have branching on the whole lateral surface (Figure 3a and c), while some of them only grew at a lateral side, as shown in Figure 3(b). Two possible paths were expected to be followed by the formation of these hierarchical NSs. By following Path A in the schematic diagram, as shown in Figure 4, surface migration has taken part. Au droplets mixed with the source material were covering the whole lateral surface of the trunk NWs and the branched NWs formed at the energetically favourable angles at all lateral sides. If Path B has been followed, the surface migration was not taking part and only the side which faces the source material has the formation of the branched NWs. The criterion for the occurrence of surface migration on the NW is still not clear up-to-date. Both types of the hierarchical structures observed in the SEM images resemble the pine-leaf shape. It could be deduced that these specific contact angles may be due to the epitaxial-like growth of SnO_2 NWs on the SnO_2 trunk NWs. A similar case has been reported by Wang et al. [25] for the growth of Si NWs. The surfaces of the branching NWs appear to be smooth, from the image, without having any bloated area on the side surface of each NW while the trunk NWs are covered with

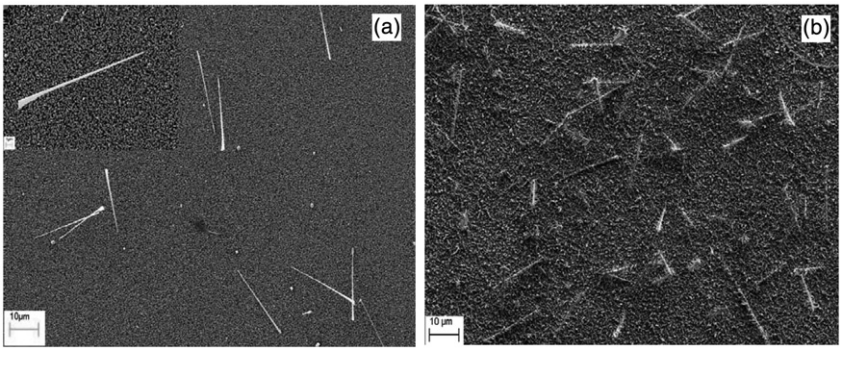

Figure 2. SEM image of SnO_2 NSs: (a) after the primary growth process – tapered NWs were formed and (b) after the secondary growth process – 3D hierarchical structure were formed.

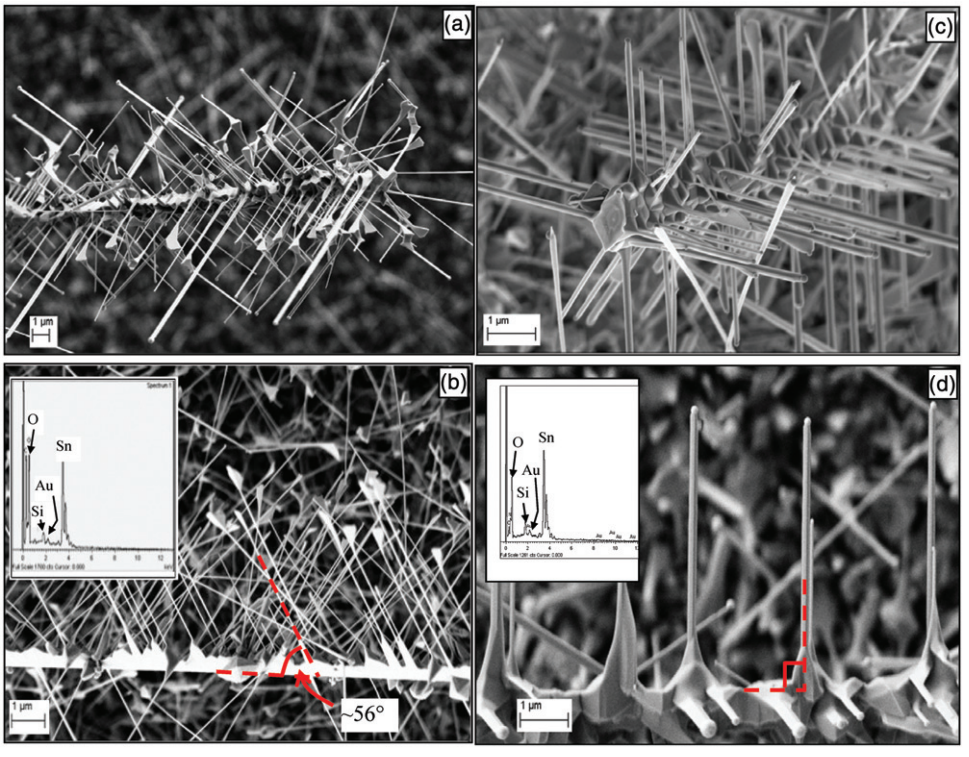

Figure 3. SEM image for the two types of 3D pine-leaf-like SnO_2 on SnO_2 NSs after the secondary growth process. (a,b) The perspective views of a hierarchical SnO_2 structure with an included angle of 56°, as shown in a lateral view (b); (c) another type with an included angle of 90°; and (d) the corresponding lateral view.

plenty of residues of SnO_2. EDX spectrum is shown as insets in Figure 3(b) and (d). The figure reveals the presence of the peak for Au element which acted as the catalyst during the growth process. Peaks for major elements of Sn and O indicate the NWs consisted of Sn and O.

Figure 5(a) shows a TEM image of a branched NW. The corresponding HRTEM has been shown in Figure 5(b). Fast Fourier transformation (FFT) has been done within the open box area marked in the figure. The estimation for the lattice width and the FFT justify a growth direction of [1 0 1] for the branched NW [5]. An angle of ~56° for the branched NW with the trunk axis provided that the trunk was growing in the direction of [1 0 0]. Theoretical calculation shows that the growth of NW at [1 0 1] on the [1 0 0] trunk will provide an included angle of 56°, which is same as the one we have obtained. A thermodynamic equation by the Wulff construction for the surface energies is shown in Equation (1) [26, 27]:

$$\Delta G = E^{A}_{\text{surf}}(h_1k_1l_1)\cos\theta - E^{B}_{\text{surf}}(h_2k_2l_2) \tag{1}$$

where $E^{A}_{\text{surf}}(h_1k_1l_1)$ is the surface formation energy per unit area for the orientation of $(h_1k_1l_1)$, $E^{B}_{\text{surf}}(h_2k_2l_2)$ the surface formation energy per unit area for the orientation of $(h_2k_2l_2)$, θ the angle between the two planes and $\cos\theta$ the effect of the increase in surface area for the new facet. Based on the calculation, the faceting change from (1 0 0) to (1 0 1) or (1 0 $\bar{1}$) will give an energy of $-0.778\,\text{J m}^{-2}$ which is thermodynamically favourable. Calculation for the faceting change from (1 0 0) to (1 1 0) is also thermodynamically stable ($-0.864\,\text{J m}^{-2}$). Due to the tetragonal

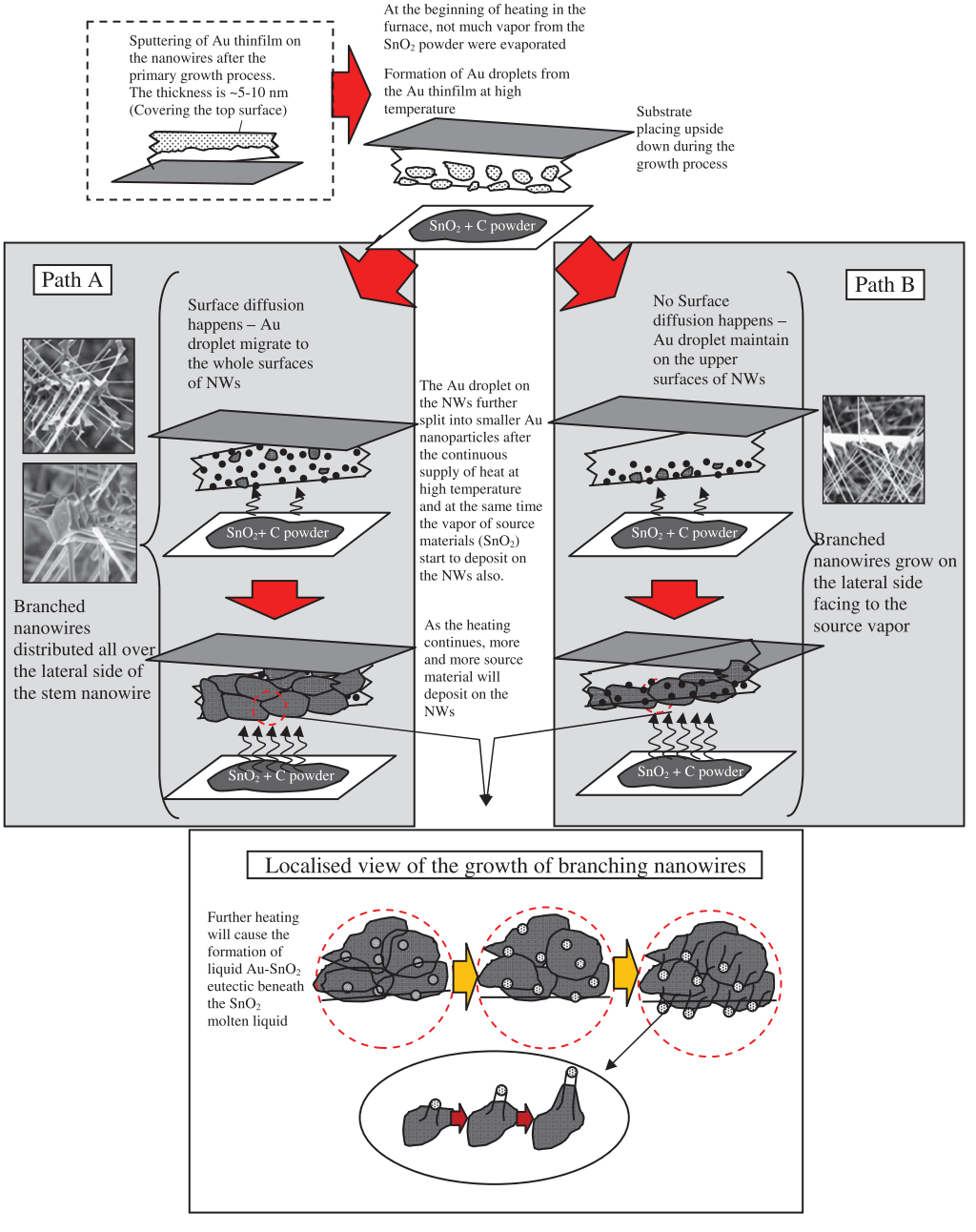

Figure 4. A schematic diagram of the two different paths followed to produce hierarchical NSs. Path A, the surface migration happened and the branched NWs distributed over the whole lateral surface and Path B, no surface migration and the branched NWs only grew on the side facing to the source vapour.

structure of the SnO_2 crystal, (1 0 1) and (1 0 $\bar{1}$) are kinetically identical in the crystal growth, similar also for facet of (1 1 0) and (1 $\bar{1}$ 0). Therefore, most of the branching is grown from these four facets ((1 0 1; (1 0 $\bar{1}$); (1 1 0); and (1 $\bar{1}$ 0)) which form a fourfold symmetry of hierarchical structure, as shown in the schematic diagrams in Figure 6. For the 90° branching from the

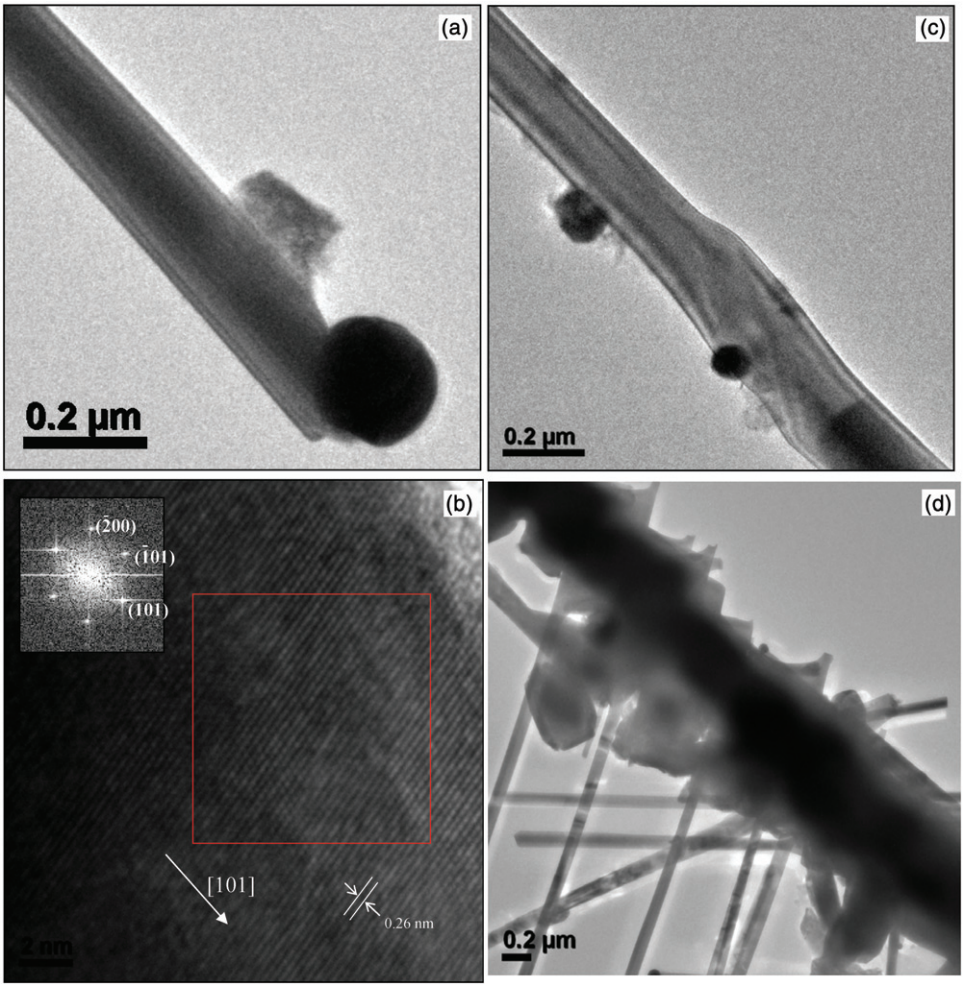

Figure 5. TEM images of the hierarchical NWs: (a) the branched NW with an Au droplet on the tip; (b) HRTEM and the FFT (inset) images of the branched NW shown in (d) that grows along the [1 0 1] direction; (c) a TEM diagram showing an initial stage where Au droplet catalysts form on the surface before the branching process; and (d) TEM image showing an angle of 56° branching from the trunk NW.

growth direction of (0 1 0), (0 0 1), (0 $\bar{1}$ 0) and (0 0 $\bar{1}$) from (1 0 0) trunk (Figure 3c), calculation gives a value of −1.648, which is also thermodynamically stable. Directions of [0 1 0] and [0 $\bar{1}$ 0] are kinetically identical in the growth of tetragonal SnO_2 crystal. It is similar also for [0 0 1] and [0 0 $\bar{1}$]. Occasionally, diagonal branching from the directions of [0 1 1], [0 1 $\bar{1}$], [0 $\bar{1}$ $\bar{1}$] and [0 $\bar{1}$ 1] are also observed, as shown in Figure 3(c).

Literature study has shown that the position of the substrate located very near the source material will eventually cause the supersaturation on the substrate before the formation of NWs [28]. This condition fulfils the criteria which is fairly common in the formation of dendritic/branching crystals in bulk crystal growth [28]. This may be one of the reasons why the formation of branched NWs was induced during the secondary growth process. The Au catalyst also plays its role in this part. The presence of Au catalyst is expected to enhance the yield of the product in

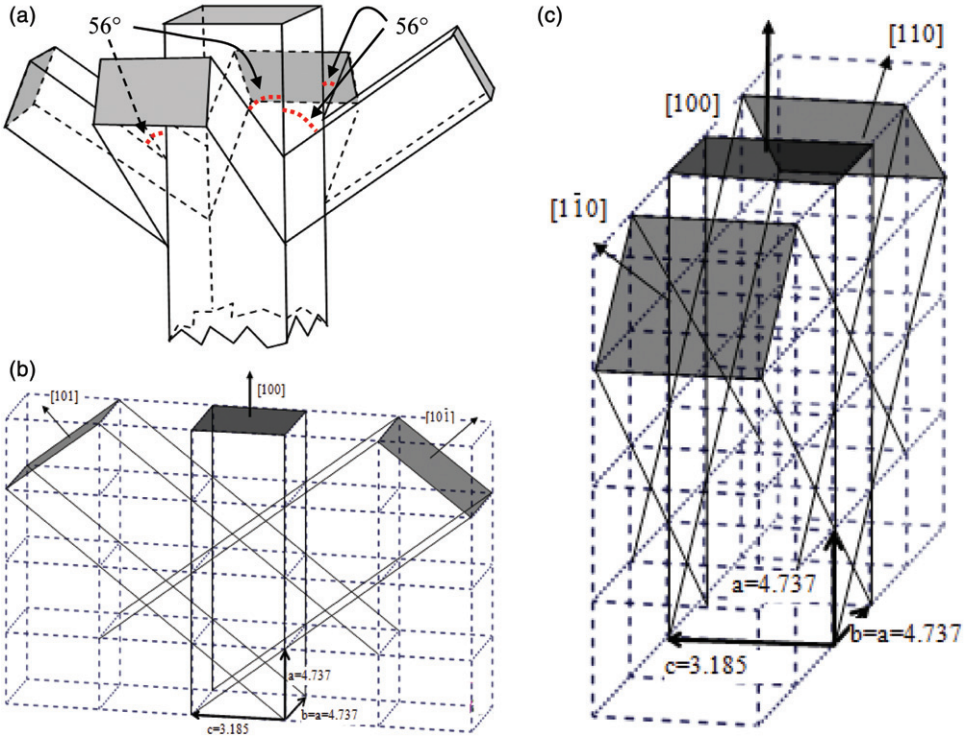

Figure 6. A schematic diagram of the 3D hierarchical NS with an included angle of ~56° (a) and the branching NWs shown separately in the directions of [1 0 1] and [1 0 $\bar{1}$] (b) and [1 1 0] and [1 $\bar{1}$ 0] (c), respectively.

this supersaturated region. In the sputtering process after the primary growth, Au thin film was deposited on the top lateral side of the horizontally laying SnO_2 NWs. Heating of this Au layer caused the formation of Au droplets, which would then reduce their sizes to smaller Au NPs when heated up at 950°C. At the same time, the source vapour (from SnO_2 powder) would also form liquid droplets which covered the lateral surface of the NWs and also the Au NPs, as shown in schematic diagram at the bottom part of Figure 4. The Au NPs on the lateral sides of SnO_2 NWs provided the energetically favoured sites and catalysed the growth process of the branching NWs by adsorption of the supersaturated SnO vapour. SnO might have decomposed, forming SnO_2 and led by the top Au catalysed to form the lateral branches of NWs. There was excessive source liquid deposited on the trunk NWs at the beginning of the growth, which would then solidify as irregular shape at the base of the branching SnO_2 NWs. Sometimes, the migration of Au droplets had not happened and the branched NWs were only formed on one site of the trunk NWs. A schematic diagram shown in Figure 4 is used to simplify the whole process described above.

Figure 7 shows the XRD spectrum for the scanning done after the primary and secondary growth processes. Highly crystalline structures have been obtained after both the primary and secondary growth processes. The peaks could be indexed to the tetragonal rutile structure of SnO_2 with lattice parameters of $a = 0.4737$ nm and $c = 0.3185$ nm, which agree well with the standard data file (JCPDS 21-1250). Evidently there is no change in the crystalline nature of the SnO_2 system before and after the secondary growth process.

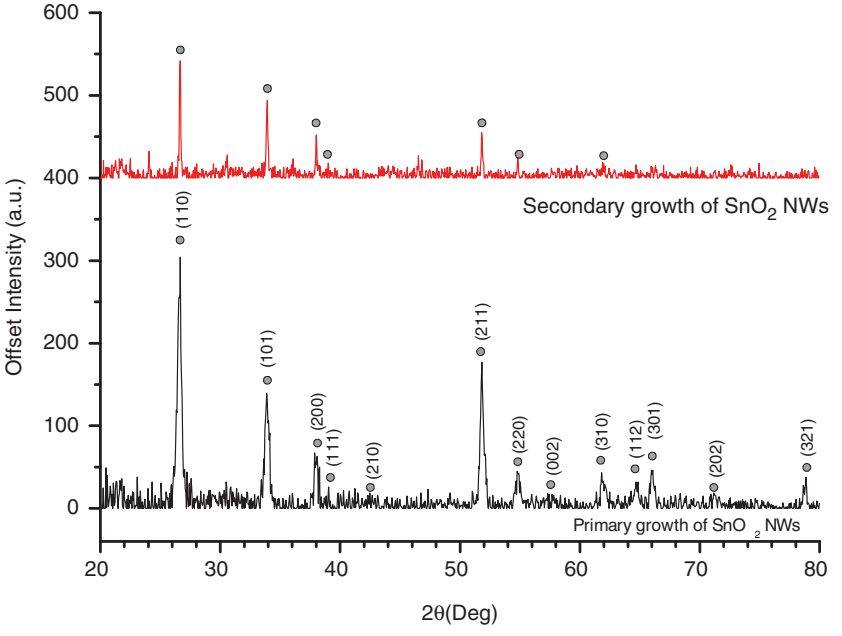

Figure 7. XRD patterns of SnO_2 NWs grown in the primary and secondary processes, respectively.

4. Conclusion

In summary, SnO_2 hierarchical NSs have been synthesised by two consecutive VTD methods. This approach has managed to reduce the time taken for switching between more than one growth processes to produce the branching NSs. The specific included angles for the formation of hierarchical NSs were justified by the thermodynamic calculation to be energetically favourable. Further control techniques for the branching NWs are needed to control the junction angle in future. This may lead to the development of interconnecting NWs for the future generation nanoelectronic devices.

Acknowledgements

This study is financially supported by University Research Grant Scheme (UKM-GUP-2011-378), (UKM-DLP-2012-033) and Fundamental Research Grant Scheme by Ministry of Higher Education, Malaysia (UKM-RRR1-07-FRGS0025-2010).

References

[1] Z.L. Wang, *ZnO nanowire and nanobelt platform for nanotechnology*, Mater. Sci. Eng. R 64 (2009), pp. 33–71.
[2] T. Sahm, W. Rong, N. Barsan, L. Madler, and U. Weimar, *Sensing of CH_4, CO and ethanol with in situ nanoparticle aerosol-fabricated multilayer sensors*, Sens. Actuators B 127 (2007), pp. 63–68.
[3] N.N. Samotaev, A.A. Vasiliev, B.I. Podlepetsky, A.V. Sokolov, and A.V. Pisliakov, *The mechanism of the formation of selective response of semiconductor gas sensor in mixture of $CH_4/H_2/CO$ with air*, Sens. Actuators B 127 (2007), pp. 242–247.
[4] Y.J. Chen, C.L. Zhu, M.S. Cao, and T.H. Wang, *Photoresponse of SnO_2 nanobelts grown in situ on interdigital electrodes*, Nanotechnology 18 (2007), pp. 1–5.
[5] J.X. Wang, D.F. Liu, X.Q. Yan, H.J. Yuan, L.J. Ci, Z.P. Zhou, Y. Gao, L. Song, L.F. Liu, W.Y. Zhou, G. Wang, and S.S. Xie, *Growth of SnO_2 nanowires with uniform branched structures*, Solid State Commun. 130(1–2) (2004), pp. 89–94.

[6] Z.J. Li, H.Y. Wang, P. Liu, B. Zhao, and Y.F. Zhang, *Synthesis and field-emmission of aligned SnO_2 nanotubes arrays*, Appl. Surf. Sci. 255(8) (2009), pp. 4470–4473.
[7] C. Nayral, E. Viala, P. Fau, F. Senocq, J.-C. Jumas, A. Maisonnat, and B. Chaudret, *Synthesis of tin and tin oxide nanoparticles of low size dispersity for application in gas sensing*, Chemistry 6 (2000), pp. 4082–4090.
[8] H.W. Kim, N.H. Kim, J.H. Myung, and S.H. Shim, *Characteristics of SnO_2 fishbone-like nanostructures prepared by the thermal evaporation*, Phys. Status Solidi A 202(9) (2005), pp. 1758–1762.
[9] F.K. Shan, B.C. Shin, S.C. Kim, and Y.S. Yu, *Characterizations of Al doped zinc oxide thin films fabricated by pulsed laser deposition*, J. Korean Phys. Soc. 42 (2003), pp. S1374–S1377.
[10] X.W. Zhu, Y.Q. Li, Y. Lu, L.C. Liu, and Y.B. Xia, *Effects of Li or Li/Mg dopants on the orientation of ZnO nanorods prepared by sol-gel method*, Chem. Phys. 102(1) (2007), pp. 75–79.
[11] C.-J. Pan, H.-C. Hsu, H.-M. Cheng, C.-Y. Wu, and W.-F. Hsieh, *Structural and optical properties of ZnMgO nanostructures formed by Mg in-diffused ZnO nanowires*, J. Solid State Chem. 180(4) (2007), pp. 1188–1192.
[12] K.L. Merkle and W. Jäger, *Direct observation of spike effects in heavy-ion sputtering*, Philos. Mag. A 44 (1981), pp. 741–762.
[13] Z. Ni, Q. Li, D. Zhu, and J. Gonga, *Fabrication of carbon nanowire networks by Si ion beam irradiation*, Appl. Phys. Lett. 89 (2006), pp. 053107-1–053107-3.
[14] Z. Ni, Q. Li, L. Yan, J. Gong, D. Zhu, and Z. Zhu, *Intensive irradiation of carbon nanotubes by Si ion beam*, Nucl. Sci. Tech. 18(3) (2007), pp. 137–140.
[15] Z. Ni, Q. Li, J. Gong, D. Zhu, and Z. Zhu, *Structural change of carbon nanotubes produced by Si ion beam irradiation*, Nucl. Instrum. Methods Phys. Res., Sect. B 260 (2007), pp. 542–546.
[16] M. Dutta and D. Basak, *Multiwalled carbon nanotubes/ZnO nanowires composite structure with enhanced ultraviolet emission and faster ultraviolet response*, Chem. Phys. Lett. 480(4–6) (2009), pp. 253–257.
[17] Y.L. Wu, A.I.Y. Tok, F.Y.C. Boey, X.T. Zeng, and X.H. Zhang, *Surface modification of ZnO nanocrystals*, Appl. Surf. Sci. 253(12) (2007), pp. 5473–5479.
[18] K.S. Choi, C.W. Ok, S.Y. Jo, K.H. Bai, and Y.H. Im, *Ion bombardment effects on the ZnO nanowires during plasma treatment*, Appl. Phys. Lett. 93 (2008), pp. 033112-1–033112-3.
[19] H. Yan, R. He, J. Johnson, M. Law, R.J. Saykally, and P. Yang, *Dendritic nanowire ultraviolet laser array*, J. Am. Chem. Soc. 125 (2003), pp. 4728–4729.
[20] D. Wang and C.M. Lieber, *Inorganic materials: Nanocrystals branch out*, Nat. Mater. 2 (2003), pp. 355–356.
[21] T.Y. Tiong, M. Yahya, C.F. Dee, K.P. Lim, B.Y. Majlis, and C.H. Sow, *Influence of growth temperature on SnO_2 nanowires*, Mater. Res. Innovations 13(3) (2009), pp. 203–206.
[22] C. Cheng, B. Liu, H. Yang, W. Zhou, L. Sun, R. Chen, S.F. Yu, J. Zhang, H. Gong, H. Sun, and H.J. Fan, *Hierarchical assembly of ZnO nanostructures on SnO_2 backbone nanowires: Low-temperature hydrothermal preparation and optical properties*, ACS Nano 3(10) (2009), pp. 3069–3076.
[23] D.C. Fu, B.Y. Majlis, M. Yahaya, and M.M. Salleh, *Electrical characterization of cross-linked ZnO nanostructures grown on Si and Si/SiO_2 substrate*, Sains Malays. 37(3) (2008), pp. 281–283.
[24] C. Ye, X. Fang, Y. Hao, X. Teng, and L. Zhang, *Zinc oxide nanostructures: Morphology derivation and evolution*, J. Phys. Chem. B, 109(42) (2005), pp. 19758–19765.
[25] D. Wang, F. Qian, Z. Zhong, and C.M. Lieber, *Rational growth of branched and hyperbarnched nanowire structures*, Nano Lett. 4(5) (2004), pp. 871–874.
[26] G. Wulff, *Velocity of growth and dissolution of crystal faces*, Z. Kristallogr. 34 (1901), pp. 449–530.
[27] C. Herring, *Some theorems on the free energies of crystal surfaces*, Phys. Rev. 82(1) (1951), pp. 87–93.
[28] J.J. Gilman, *The Art and Science of Growing Crystals*, John Wiley and Sons, New York, 1963.